Temperature-Modulated Doping at Polymer Semiconductor Interfaces

Natalie P. Holmes[1,2▲*], Daniel C. Elkington[1▲], Matthew Bergin[1], Matthew J. Griffith[1,3], Anirudh Sharma[4,5], Adam Fahy[1], Mats R. Andersson[4], Warwick Belcher[1], Jakub Rysz[6], Paul C. Dastoor[1]

[1] Centre for Organic Electronics, University of Newcastle, Callaghan, NSW 2308, Australia

[2] Australian Centre for Microscopy and Microanalysis, University of Sydney, Madsen Building F09, NSW 2006, Australia

[3] School of Aerospace, Mechanical and Mechatronic Engineering, University of Sydney, NSW 2006, Australia.

[4] Flinders Institute for Nanoscale Science and Technology, Flinders University, Sturt Road, Bedford Park, Adelaide, SA 5042, Australia

[5] King Abdullah University of Science and Technology (KAUST), Physical Sciences and Engineering Division (PSE), KAUST Solar Center (KSC), 23955, Thuwal, Saudi Arabia

[6] Institute of Physics, Jagiellonian University, 30-059 Kraków, Poland

* Corresponding author, natalie.holmes@sydney.edu.au

▲ These authors contributed equally.

Keywords

Biosensor, printed electronics, organic electronics, doping, semiconductor interface

Abstract

Understanding doping in polymer semiconductors has important implications for the development of organic electronic devices. This study reports a detailed investigation of the doping of the poly(3-hexylthiophene) (P3HT)/Nafion bilayer interfaces commonly used in organic biosensors. A combination of UV-visible spectroscopy, dynamic secondary ion mass spectrometry (d-DIMS), dynamic mechanical thermal analysis (DMTA) and electrical device characterization reveal that the doping of P3HT increases with annealing temperature and this increase is associated with thermally activated interdiffusion of the P3HT and Nafion. First principles modelling of d-SIMS depth profiling data demonstrates that the diffusivity coefficient is a strong function of the molar concentration; resulting in a discrete intermixed region at the P3HT/Nafion interface that grows with increasing annealing temperature. Correlating the electrical conductance measurements with the diffusion model provides a detailed model for the temperature-modulated doping that occurs in P3HT/Nafion bilayers.

Point-of-care testing has created a market for low-cost sensor technology, with printed organic electronic sensors well positioned to meet this demand, and this article constitutes a detailed study of the doping mechanism underlying such future platforms for the development of sensing technologies based on organic semiconductors.

1. Introduction

Organic electronics is an attractive platform for the development of low-cost printed sensors. Their suitability for such applications is due to the solution processability of organic semiconductors and thus the applicability of conventional printing techniques to fast and automated printing manufacture.[1] Indeed, a number of roll-to-roll (R2R) printing techniques have already been demonstrated for organic electronic device fabrication including slot-die coating,[2] flexographic printing,[3] and screen printing.[4] A second key advantage of organic electronics over their inorganic counterparts is their biocompatibility, which enables such devices to be seamlessly interfaced with biological systems such as enzymes.[5–7]

The sensing mechanism in organic electronic sensors commonly involves altering the doping of semiconducting polymers; resulting in a measurable change in device response to the analyte.[8,9] The doping of thiophene-based semiconductors by both protic and aprotic (Lewis) acids has been investigated previously, with two main pathways proposed. In both cases, doping occurs via proton transfer, either directly from the acid functionality or via a water-complex intermediary.[10] It has been proposed that the proton transfers either onto the sulphur[11,12] or the conjugated polymer backbone;[10] creating a delocalized positive charge across the semiconducting polymer that increases conductivity dramatically (Figure 1). Mauger *et al.*[11] and Nam *et al.*[12] reported the doping of P3HT by polysulphonic acids, polystyrene sulfonic acid (in two forms, namely PSS and PEDOT:PSS) and Nafion, and 2-ethylbenzenesulfonic acid, respectively. Whilst Yurash *et al.*[10] reported the doping of multiple donor polymers (each with a thiophene unit forming a core component of the polymer backbone) by a range of Lewis acid dopants. It has also been shown by Kaake, Frisbie and coworkers[13] that electrochemical mixing and associated doping occurs at the polymer interface of P3HT and the polymer electrolyte dielectric consisting of lithiumpoly(styrene sulfonate) (LiPSS) dissolved in poly(ethylene oxide) (PEO). They reported that for $V_G < -1.8$ V the density of injected charge rises rapidly until the entire P3HT:LiPSS:PEO volume is electrochemically mixed, reaching a maximum charge density of $2 \times 10^{14}/cm^2$. It is possible, and indeed likely, that entrapped oxygen and/or water may also participate in the doping of the

semiconducting polymer, especially when the materials are heated above their T_gs. In particular, light induced, irreversible interfacial oxygen doping of P3HT is a well-established phenomenon under aerobic conditions.[14]

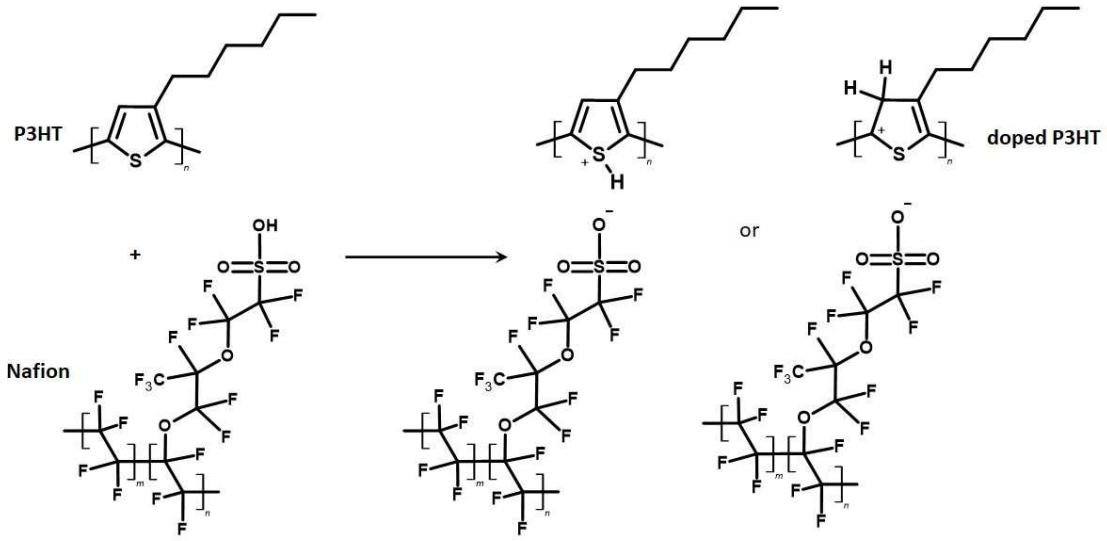

Figure 1. Chemical structure of P3HT, Nafion, and doped P3HT.

Although the chemistry of the interfacial doping mechanism is broadly understood, little is known about the structure of the doped interface or how it changes as a function of temperature. In particular, thermally activated interdiffusion alters the structure and morphology of interfacial layers and is, therefore, highly relevant to organic electronic technologies where annealing is a common processing tool. Consequently, understanding the role that thermally induced interdiffusion plays in determining interfacial structure and its subsequent impact on electrical characteristics is crucial to the design of organic electronic devices.

Here we probe the doping mechanism in as-spun and thermally annealed poly (3-hexylthiophene) (P3HT)/Nafion bilayer films, which are commonly used in organic thin film transistor (OTFT)-based sensors. UV-visible spectroscopy, electrical conductance, X-ray photoelectron spectroscopy (XPS), dynamic secondary ion mass spectrometry (d-DIMS) depth profiling and dynamic mechanical thermal analysis (DMTA) measurements have been used to develop a model for the doping and interdiffusion behaviour of the two materials as a function of thermal treatment. By modelling the system, both analytically and numerically, we show that the dependence of the conductivity of the bilayer structure upon thermal annealing

temperature involves the creation of distinct intermixed and interfacial doping regimes; explaining the observed complex evolution of conductivity.

2. Methods

2.1 Materials

P3HT was synthesized at the Centre for Organic Electronics, University of Newcastle, Australia as described by Holmes *et al.*,[15] with an M_n of 23,100 g mol^{-1}, M_w of 32,100 g mol^{-1} and PDI of 1.39 as measured by gel permeation chromatography (GPC) using polystyrene standards. The P3HT molecular weight determination was performed on an Agilent PL-GPC 220 integrated GPC system, equipped with a refractive index (RI) detector and a viscometer. The measurements were performed at 150 °C at a flow rate of 1 mL min^{-1} with 1,2,4-tricholobenzene (TCB) stabilized with 0.0125% BHT (dibutylhydroxytoluene**)** as the eluent. The polymer was separated on 3 Agilent PLgel 10 μm MIXED-B LS columns. Prior to the measurements, the polymer was dissolved in TCB at a concentration of 1 mg mL^{-1}, heated to 140 °C in the Agilent PL-SP 260VS Sample Preparation System for 1 h and thereafter filtered through a 2 μm stainless steel filter. Following filtration, the polymer was transferred immediately to the GPC. Nafion® 1100EW solution (5 wt. % in lower aliphatic alcohols and water) was purchased from Sigma Aldrich, where EW, equivalent weight, is the number of grams of dry Nafion per mole of sulfonic acid groups (chemical structure provided in Figure 1).

2.2 Electronic Device Fabrication and Characterization

For electrical characterization of Nafion/P3HT bilayers, glass substrates with sets of pre-patterned indium-doped tin oxide (ITO) electrodes (15 Ω $□^{-1}$, Xinyan Technology Limited, Figure S1a) were first cleaned by a process of sonication in, sequentially, detergent solution (Liquid Pyroneg, Diversey; 1 % by volume in purified water), purified water (Milli-Q® Direct Water Purification System, 18.2 Ω cm) and isopropyl alcohol (VWR International). The channel between the ITO electrode pairs was 20 μm long and 3 mm wide. P3HT was then spin coated from a 20 mg mL^{-1} chloroform solution at 2000 rpm and 1596 rpm s^{-1} for 60 s and dried at 50 °C for 10 min. A Nafion solution (used as received) was spin-coated at 500 rpm and 399 rpm s^{-1} for 120 s. This bilayer was subsequently annealed at a range of temperatures from 50 °C to 250 °C for 5 min. Pristine P3HT and Nafion films were also prepared on the ITO electrodes using the same deposition conditions. The thicknesses of the P3HT and Nafion films were approximately 100 nm and 370 nm, respectively. Using two medium-power source

measurement units of a Keysight B1500A semiconductor device analyzer (connected to the pairs of ITO electrodes for the bilayer structures through a Micromanipulator 450PM probe station), voltage was scanned from -0.5 V to +0.5 V in intervals of 10 mV and the current measured at each potential. The conductance (G) of the bilayer structure was calculated by applying a linear fitting algorithm to the current-voltage (IV) data and using Equation 1.

$$G = \frac{I}{V} \quad (1)$$

2.3 d-SIMS Profiling

Organic electronic devices were fabricated for d-SIMS measurements as per the protocol described in section 2.2. d-SIMS depth profiles, with a depth interval of 5 nm, were obtained using a TOF-SIMS 5 system (ION-TOF GmbH, Muenster, Germany) with 2 m time of flight mass spectrometer. A 20 keV beam of C_{60} was used to remove material by sputtering a 500 μm x 500 μm region while a 30 keV pulsed beam of Bi_3^+ cluster ions was used to analyze the composition of the central 100 μm x 100 μm area in that region. Bi_3^+ cluster ions are reported to provide better surface sensitivity for low mass fragments.[16] Secondary ions with mass to charge ratios corresponding to C^-, O^-, Si^-, CF^-, $^{34}S^-$ and In^- were collected. We chose the In^- signal as representative of ITO because the intensities of the InO^- and InO_2^- signals in our experiment were so high that they saturated the detector. The d-SIMS depth sputtering rate is calibrated from the sputter time using known depths of the individual layers. The CF^- ions (unique to Nafion) are representative of the Nafion film, the $^{34}S^-$ ions (present in both P3HT and Nafion, but at a higher fractional composition in P3HT) monitor when the P3HT bilayer film or intermixed interface region is reached, while In^- ions are an indicator of the ITO electrodes. The d-SIMS data was collected at a sampling rate of 1 point per 1.6 s.

2.4 Thermomechanical Analysis

DMTA measurements were performed to determine material glass transition temperature (T_g) on a TA Q800 DMA in strain-controlled mode with an amplitude of 5 μm, frequency of 1 Hz, temperature range of -110 to 300 °C, temperature ramp of 3 °C min^{-1}, and under a nitrogen atmosphere (60 mL min^{-1}). In order to remove possible moisture from the samples, the first scan was run from room temperature to 30 °C. Samples were prepared by drop-casting Nafion solution onto a woven glass fibre mesh substrate cut at an angle of 45° to the direction of load. Generally, the experimental setup was in accordance with that reported by Sharma *et al*.[17]

2.5 XPS and UV-Vis Characterization

For ultraviolet-visible (UV-vis) absorbance spectroscopy measurements, samples were prepared using the same conditions as for the electrical characterization measurements, with the exception of the substrate (which was plain glass instead of ITO-glass), and the samples were heated for periods of 5 min at temperatures from 50 °C to 250 °C. The UV-vis absorption spectra of the samples were measured using a Varian Cary 6000i UV-Vis-NIR spectrophotometer from λ = 1800 nm to λ = 300 nm.

For X-ray photoelectron spectroscopy (XPS) characterization, the bilayer structure was again prepared on a plain glass substrate. The Nafion layer was first deposited by spin-coating using the same conditions as for the electrical characterization and annealed for 5 min at 50 °C. Subsequently, the P3HT layer was deposited by spin coating from a 2 mg mL^{-1} chloroform solution at 2000 rpm and 1596 rpm s^{-1} for 60 s, for a nominal P3HT layer thickness of 10 nm. Importantly, note the reverse order of the deposition of Nafion and P3HT to form the bilayer structures. Samples were mounted to the XPS sample holder with conductive carbon tape, with no direct grounding applied. XPS spectra were collected by illuminating the samples with a non-monochromatic X-ray source (Omnivac) using Al Kα (1486.6 eV) radiation, and the photoemission collected by an SES2002 analyzer (Scienta). Survey scans were carried out with a pass energy of 200 eV, while region scans were performed using a pass energy of 20 eV and 100 meV steps. Pristine samples used a 10 eV pass energy. Working pressure in the analysis chamber with sample under X-ray illumination was typically 5.0 x 10^{-9} mbar, with a base pressure of 4 x 10^{-10} mbar.

3. Results and Discussion

To probe the detailed nature of polythiophene doping at the P3HT/Nafion interface, UV-visible spectra were acquired in the visible and near infrared spectral region for P3HT/Nafion bilayer films prepared at annealing temperatures ranging from 50 to 250 °C (Figure 2). Thermal annealing of the bilayer films is observed to induce two new broad peaks not previously observed in the pure P3HT films. The first peak (~ 780 nm) increases systematically with annealing temperature, with a corresponding decrease in the main P3HT absorbance peak (~ 540 nm) observed as the new peak grows. The tail of a second absorption peak (which also increases systematically with annealing temperature) occurs between 1200 nm and 1800 nm. A clear change in color of the films is detectable by eye, from purple through to green, from 50 to 250 °C, as shown in optical images (Figure S1b-f). This behaviour is consistent with the optical signatures of a P3HT bipolaron[18,19] and polaron species,[19,20] both of which are indicative of a doped P3HT polymer backbone. Furthermore, the optical signatures of these doped species

are completely absent from both the pure P3HT and pure Nafion films subjected to the same thermal annealing treatments (Figure S2) and consistent with the polaron and bipolaron bands observed for P3HT oxidatively doped with $FeCl_3$ (Figure S3 and associated text).[21] The absence of polaron and bipolaron peaks in the pure P3HT film UV-Vis spectra (Figure S2) also confirms that the role of oxygen doping (from the presence of air) is minimal and undetectable, hence we can assign the doping in the P3HT/Nafion bilayer devices to the protic doping from the interaction with Nafion.

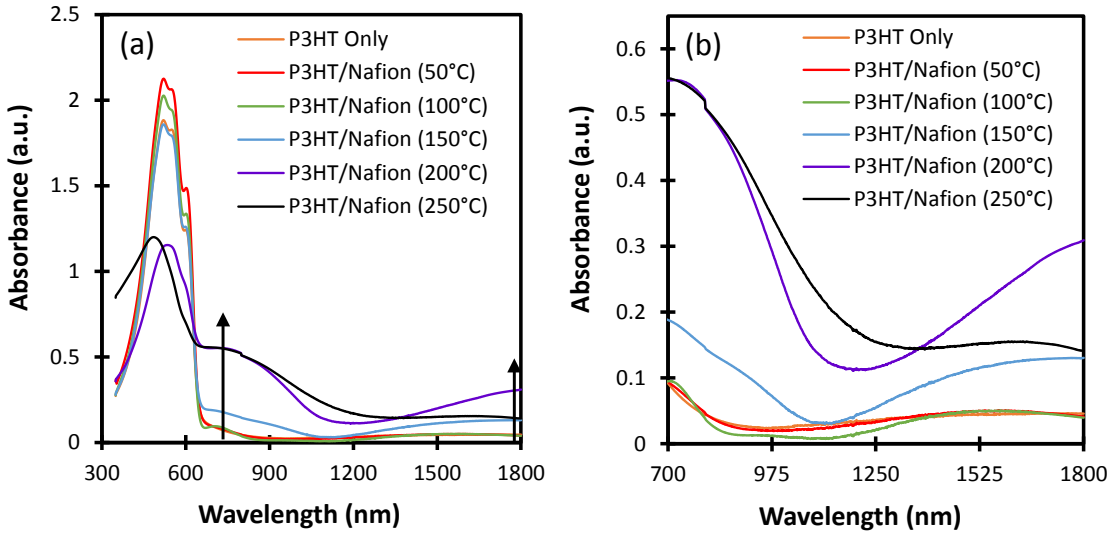

Figure 2. UV-vis absorbance spectra as a function of wavelength for pristine P3HT and P3HT/Nafion bilayers annealed at temperatures from 50 °C to 250 °C. (a) Wavelength range from 300 to 1800 nm. (b) Wavelength range from 700 to 1800 nm. The arrows highlight the increasing P3HT bipolaron (~1800 nm) and polaron (~770 nm) peaks.

XPS measurements were undertaken as a preliminary check for intermixing of the two species at the selected thermal annealing conditions. The shallow analysis depth of XPS (< 10 nm) required that the Nafion layer was deposited before the P3HT layer (~10 nm) to ensure that any degree of intermixing caused by annealing of the bilayer could be detected by XPS analysis. Figure S4 shows the survey scan for the bilayer device annealed at 200 °C and a summary of the XPS data for pristine Nafion, pristine P3HT and P3HT/Nafion films after thermal treatments of 50, 100, 200 and 250 °C. Additional survey scans are presented in Figure S5. The pristine P3HT and Nafion films exhibit characteristic photoelectron emission signals at 163.2 eV (S 2p) and 684.8 eV (F 1s), respectively. Hence, the P3HT S 2p:Nafion F 1s ratio provides a measure of the concentration of the two materials in the 10 nm surface region of the annealed bilayers. As such, Figure S4b reveals that the XPS data for bilayers annealed at 50 °C and 100

°C is consistent with a surface composition that is primarily P3HT. By contrast, the XPS data for bilayers annealed at 200 °C and 250 °C is consistent with a surface composition that is now dominated by Nafion; suggesting that Nafion interdiffusion into the P3HT has occurred. While the thermodynamic drive for Nafion to move to the air-interface (for these thin P3HT surface films) is consistent with the lower relative surface energy of Nafion (17.5 mJ m^{-2})[22] compared to that of P3HT (26.9 mJ m^{-2}),[23] this interdiffusion is only activated for temperatures above 100 °C.

In order to shed light on the intermixing of Nafion and P3HT at the bilayer interface, the T_g of Nafion was measured with DMTA. Following deposition of Nafion onto the woven glass fibre mesh substrate and drying, a sinusoidal stress was applied to the sample. The DMTA data for Nafion is presented in Figure S6, the peak temperature in tan δ was taken to represent material T_g, where tan δ = E''/E' and E' is the storage modulus and E'' is the loss modulus. Consistent with Sharma *et al.*[17] we have utilized the tan δ peak to define the T_g of Nafion. We observed two tan δ peaks, 114 °C and 233 °C. The tan δ peak at 233 °C is accompanied by an increase in E' and is hence likely due to a crosslinking interaction of the Nafion sulfonate side groups. Thus, we assign the first peak at 114 °C to the T_g of Nafion, which is consistent with the literature and attributed to the mobility of the PTFE backbone.[24] The observation of a T_g at 114 °C is in good agreement with the XPS data, which identifies that Nafion interdiffusion into P3HT is activated above 100 °C.

To quantify P3HT/Nafion intermixing as a function of annealing temperature, d-SIMS depth profiles were measured for P3HT/Nafion bilayer devices annealed at 50, 100, 150 and 250 °C (Figure 3). For annealing temperatures up to 150 °C, we can identify four distinct material zones with depth: (i) a Nafion layer (characterized by high O^- and CF^- signals), (ii) a P3HT layer (characterized by high C^- and $^{34}S^-$ signals), (iii) a ITO layer (characterized by a high In^- signal) and (iv) an intermixed region at the P3HT/Nafion interface (characterized by a change in gradient of the O^-, CF^-, C^- and $^{34}S^-$ signals) whose width increases upon annealing and is most marked at 150 °C. At an annealing temperature of 250 °C, we observe a completely intermixed P3HT/Nafion film with the disappearance of the bilayer interface.

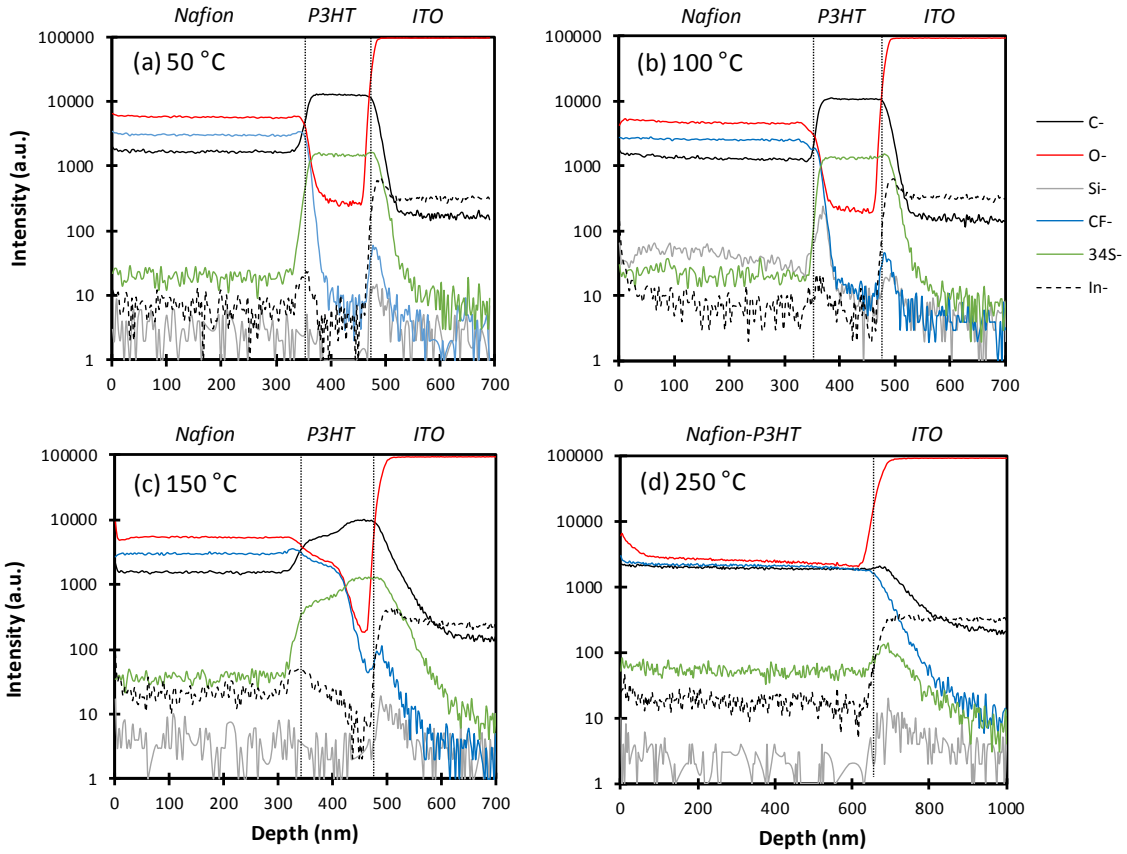

Figure 3. d-SIMS depth profile for organic electronic devices of architecture glass/ITO/P3HT/Nafion, annealed at (a) 50 °C, (b) 100 °C, (c) 150 °C, and (d) 250 °C for 5 min. Three zones are identified in (a-c) as Nafion, P3HT and ITO; whereas two zones are identified in (d) as Nafion-P3HT and ITO. Designation of the top and bottom of each layer in the device has been noted with dotted lines and this interpretation is based on changes in signal intensity consistent with similar interpretation of d-SIMS data by Hansson *et al.*[25]

Figure 4a and 4b show an expanded view of the O^- and the CF^- mass intensity depth profiles at the three annealing temperatures in the region of the P3HT/Nafion interface, respectively. In this region, the O^- and the CF^- mass signals are primarily associated with the Nafion component of the film and thus transition from high to low intensities as the P3HT/Nafion interface is crossed (~120 nm from the ITO/P3HT interface). The vertical dotted lines in the plots are located at the 80 % and 20 % levels of the interfacial step height for both the O^- and the CF^- signals; defining here the width of the interface (Table 1). In both the O^- and the CF^- signals there is: (i) a broadening of the interfacial region and (ii) an evolution of a clear inflexion in the mass signal, as the annealing temperature increases from 50 °C to 150 °C.

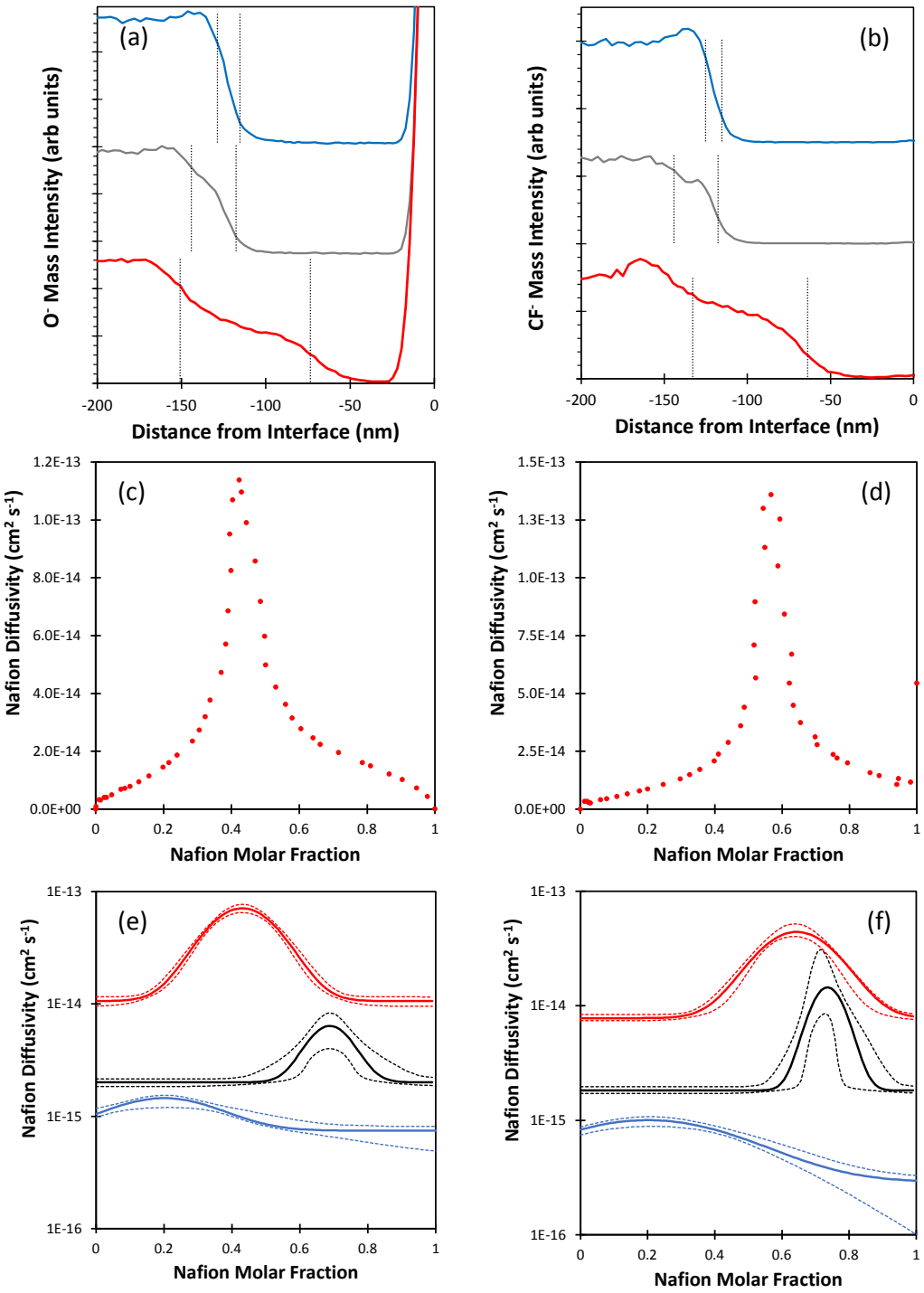

Figure 4. (a) and (b) Stacked O^- and CF^- depth profiles for glass/ITO/P3HT/Nafion samples annealed at 50 °C (blue line), 100 °C (grey line), 150 °C (red line), where the depth scale has been referenced to the P3HT/ITO interface, which is essentially invariant in all of the profiles. The vertical dotted lines are located at the 80% and 20% levels of the interfacial step height for both the O^- and the CF^- signals, defining the interface width. (c) and (d) Diffusion constant as a function of relative concentration of the Nafion component obtained by fitting the O^- mass intensity and CF^- mass intensity for the bilayers annealed at 150 °C using the Sauer and Freise (SF) method. (e) and (f) Diffusion constant as a function

of relative concentration of the Nafion component obtained by numerically modelling the O^- mass intensity and CF^- mass intensity profiles, respectively.

Examining Figure 4a and Figure 4b in more detail reveals that the direction of the broadening changes with annealing temperature. Initially, the interfacial region moves into the Nafion layer as the annealing temperature is increased from 50 °C to 100 °C (indicating that P3HT is the dominant mobile species), but then appears to move into the P3HT layer as the annealing temperature is increased from 100 °C to 150 °C (indicating that Nafion has now become the dominant mobile species). These observations are consistent with the respective T_g values of P3HT (38 °C)[17] and Nafion (114 °C); predicting that at 50 °C and 100 °C the P3HT species is the primary mobile species whereas at 150 °C the Nafion species is mobilized.

Table 1. P3HT/Nafion interface widths measured from the O^- and the CF^- depth profiles

Annealing Temperature (°C)	O^- interface width (nm)	CF^- interface width (nm)
50	13	12
100	25	27
150	82	80

Simple Fickian interdiffusion of P3HT and Nafion would manifest in the depth profiles as a smooth exponential-like change in the O^- and the CF^- mass signals between the two pure materials.[26] By contrast, the observation of an inflexion in the mass intensity plots as a function of depth in the interfacial region indicates that the diffusion of the two materials is non-Fickian and is consistent with a variable diffusivity that is higher in the mixed region.[26] As a consequence, a new distinct mixed phase between the P3HT and Nafion is created; bounded by interfaces with the pure materials. In order to understand the time-dependent formation of this new phase the interdiffusion process needs to be modelled mathematically. Specifically, the one-dimensional diffusion equation is given by:

$$\frac{\partial C(x,t)}{\partial t} = \frac{\partial}{\partial x}(J(x,t)), \quad (1)$$

with the solution given by:

$$J(x,t) = D(C)\frac{\partial C(x,t)}{\partial x}, \quad (2)$$

where C is the concentration, J is the flux and $D(C)$ is the diffusivity which varies with concentration.

Assuming that the d-SIMS signal is linearly related to the concentration of the diffusing species, the depth profile can be fitted using the Sauer and Freise (SF) method[27] taking into account the relative molar volumes of the two species.[28] Using this approach, the diffusivity, D, is expressed as a function of molar fraction, χ, such that:

$$D(\chi^*) = -\frac{V_m}{2t}\left(\frac{dx}{d\chi}\right)\Bigg|_{\chi^*}\left[\chi^*\int_{-\infty}^{x^*}\frac{(1-\chi)}{V_m}dx + (1-\chi^*)\int_{x^*}^{+\infty}\frac{\chi}{V_m}dx\right] \quad (3)$$

where V_m, t, and x are the molar volume, annealing time and depth, respectively. The molar volume can be approximated by applying Vegard's law to the monomer molar volumes of P3HT (151 $cm^3\ mol^{-1}$)[29] and Nafion (537 $cm^3\ mol^{-1}$)[30].[28]

To a first approximation, the depth profiles can be fitted with a high order polynomial; enabling the gradient term ($dx/d\chi$) to be obtained analytically. This approach was applied to the O^- and CF^- mass intensity data for the bilayers annealed at 150 °C, since these depth profiles exhibit the most marked inflexions. The resulting diffusivity plots as a function of molar fraction (Figure 4c and Figure 4d) exhibit roughly symmetric peaked distributions with diffusion coefficient values ranging from ~10^{-14} $cm^2\ s^{-1}$ in the pure materials to ~10^{-13} $cm^2\ s^{-1}$ in the mixed phase, with the maximum occurring at a Nafion molar fraction of 0.42 and 0.57 for the O^- and CF^- signals, respectively. These diffusion coefficient values are in agreement with the expected values (10^{-13} – 10^{-15} $cm^2\ s^{-1}$) for interdiffusion of polymer films annealed above their T_g.[31]

Moreover, the shift in the O^- diffusivity peak position to an apparently lower Nafion mass fraction can be explained by the presence of water molecules associated with the Nafion head groups. Whereas the CF^- signal originates uniquely from the Nafion species, the normalized O^- mass signal arises from both Nafion and water molecules associated with the hydrated film. The number of water molecules per sulphonate group is known to vary with relative humidity (RH); ranging from 1 – 14 for a RH from 0 – 100 %.[32] Given that the Nafion in this study contains 5 oxygen atoms per head group and that the SIMS analysis occurs in vacuo it seems reasonable to assume that there are probably 1 – 2 additional oxygen atoms per head group due to the water of hydration. As such, in the bulk Nafion phase there are 6 – 7 oxygen atoms per sulphonate group, whereas in the intermixed phase this number decreases to 5 oxygen atoms per sulphonate group, with only partial ingress of associated water into the hydrophobic P3HT phase occurring. Consequently, the O^- diffusivity peak decreases to an apparent Nafion molar fraction between 0.47 and 0.40; in good agreement with the measured value of 0.42. The

observation that oxygen is excluded from the expanding intermixed region, rather than drawn into it, strongly suggests that O_2 doping of the P3HT plays a minor role in the changes to conductivity which are detected, supporting the hypothesis that protic doping is the major contributor to the conductivity change in the intermixed region.

For temperatures below the T_g of Nafion fitting the depth profile becomes problematic since the intermixing behavior of the bilayer becomes much less pronounced. Consequently, in order to obtain a robust determination of the diffusivity across the entire temperature range, the diffusion across the interface has to be modelled numerically. Based on the SF model results, the diffusivity was parameterized in terms of a Gaussian function:

$$D(\chi) = \alpha + \frac{\gamma}{\sqrt{2\pi}\beta}\exp\left(-\frac{(\chi-\chi_0)^2}{2\beta^2}\right) \quad (4)$$

where α,β,γ and χ_0 are variables to be optimized.

A forward time, centered space method was used to numerically solve the diffusion equation at discrete points and take a linear interpolation to obtain estimates for the d-SIMS signal. A non-linear least-squares fitting was used to determine the optimum values of the variables, while the error in the diffusivity was determined by executing the numerical analysis for a range of values around the optimized variables and using a Bayesian approach to estimate the width of the probability distribution at each value of the optimal diffusivity.[33] The influence of discontinuous changes in calibrated depth sputter rate was assessed by performing the analysis on data sets where the calibrated change in sputter rate was placed at an arbitrary position away from each interface. However, the effect on the modelled diffusivity was small, particularly for the high temperature data where there was still clear evidence of a varying diffusivity across the interface.

The results of the numerical analysis for the O^- and the CF^- mass intensity depth profiles at the three annealing temperatures are shown in Figure 4e and Figure 4f. The plots for the 150 °C depth profiles are in good agreement with the SF method results; reproducing the positions of the O^- and the CF^- diffusivity distributions. The numerical analysis also shows that the diffusivity peak decreases in amplitude and shifts to higher Nafion molar fractions as the annealing temperature decreases from 150 °C to 100 °C; consistent with the intermixing process now limited to P3HT diffusion into the Nafion phase. As the annealing temperature decreases further from 100 °C to 50 °C the numerical analysis is unable to determine definitively a variable diffusivity.

Electronic devices consisting of P3HT/Nafion bilayers on ITO electrodes were constructed in order to determine the electrical conductivity of the films (and hence the degree of P3HT doping) as a function of annealing temperature. Figure 5a shows the electrical conductance of: (a) pristine P3HT, (b) pristine Nafion and (c) P3HT/Nafion bilayers as a function of annealing temperature. Two-probe measurements were performed on devices with constant dimensions (the same architecture), making the electrical measurements comparable within and between datasets. The conductance of both pristine P3HT and Nafion is ~ 5 x 10^{-8} S at room temperature and for annealing temperatures up to around 125 °C, whereupon the conductance of P3HT decreases gradually (~10^{-8} S) and then substantially above 175 °C (~10^{-9} S). The conductance of the Nafion films does not vary significantly over the full range of temperatures studied. Notably, the conductance of the P3HT/Nafion bilayer film at room temperature (with no thermal treatment applied) is three orders of magnitude higher (~10^{-5} S) than that of either of the single component films, this conductance increases monotonically with annealing temperature up to ~ 150 °C, whereupon the conductance plateaus (> 10^{-4} S), before decreasing dramatically at an annealing temperature of 200 °C. The observation of substantial P3HT doping upon contact with Nafion, and formation of a bilayer interface, is consistent with similar rises in conductivity observed for P3HT-based transistor devices doped with dodecyl benzene sulfonic acid reported by Alveroglu *et al.*[34] Using the method detailed in the Supporting Information (page S-5 to S-6), the conductivity of the doped, intermixed region of the P3HT/Nafion bilayer was determined to be 7.71 ± 0.86 S cm^{-1} across an annealing temperature range of 25 °C to 175 °C; an increase from the estimated conductivity of the neat P3HT film annealed at 25 °C of 3.23 ± 0.14 x 10^{-5} S cm^{-1}. These conductivity values align well with those reported elsewhere for doped and undoped P3HT films.[35,36]

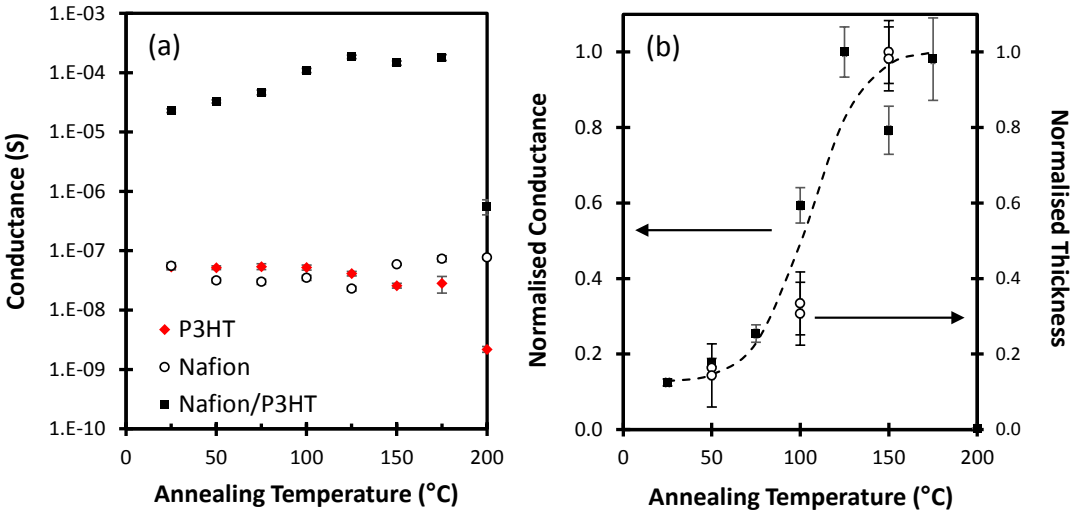

Figure 5. (a) Electrical conductance of P3HT single layer (filled red diamonds), Nafion single layer (open circles) and P3HT/Nafion bilayer devices (filled black squares) annealed at temperatures from 50 °C to 200 °C. In each case, datapoints represent the average of measurements across four samples and the error bars are ± σ. The data points corresponding to 25 °C represent room temperature (no further annealing post material deposition). (b) Electrical conductance of P3HT/Nafion bilayer devices (filled black squares) and the thickness of their intermixed regions (open circles) from Table 1, each normalized to the maximum value in each series, presented as a function of annealing temperature from 50 °C to 200 °C. The data point corresponding to 25 °C represents room temperature (no further annealing post material deposition). The dashed line represents a sigmoidal fit to the data and demonstrates a strong correlation between the two data sets up to 175 °C.

The diffusion modelling work shows that the diffusivity depends on the molar composition; resulting in the formation of a discrete intermixed region with defined boundaries. Correlating this result with the electrical conductivity measurements suggests that the observed increase in conductivity upon annealing is directly related to the formation of this discrete P3HT/Nafion intermixed region. Figure 5b plots the normalized conductivity and interlayer thickness as a function of annealing temperature. The data reveals that there is a good qualitative agreement between the two datasets; indicating a linear relationship between the conductance and the thickness of the P3HT/Nafion intermixed region. Thus, increased thermal annealing of P3HT/Nafion bilayers results in interdiffusion of the two materials and consequently the growth of a bulk-doped intermixed three-dimensional volume of enhanced conductivity. This process is in contrast to the observed doping at room temperature, which is limited to the two-dimensional bilayer interface between the two materials. From Figure 5b, this doped interfacial region is ~ 10 nm thick, which we speculate arises from ion-pairing and roughness at the interface rather than any physical intermixing.[37] Upon thermal annealing at 150 ºC for 5 minutes, the normalized thickness of the intermixed phase increases tenfold, in excellent agreement with the commensurate increase in electrical conductance. This observation is

consistent with the proportionate increase of a doped mixed phase. Finally, between 175 ºC and 200 ºC, a breakdown in the electrical properties of the P3HT/Nafion material system occurs indicating a drastic change in compositional state, consistent with the d-SIMS depth profile observed at 250 ºC.

Figure 6 summarizes the processes that occur during the thermal treatment of the P3HT/Nafion bilayer. Upon deposition of Nafion onto P3HT, a ~ 10 nm thick H^+ doped P3HT region forms at the P3HT/Nafion interface. At annealing temperatures above the T_g of P3HT (38 °C) the P3HT becomes mobile and diffuses into the Nafion; forming a new intermixed and bulk doped region. At annealing temperatures above the T_g of Nafion (114 °C) the Nafion becomes mobile and now diffuses back into the P3HT, greatly expanding the thickness of the doped intermixed region.

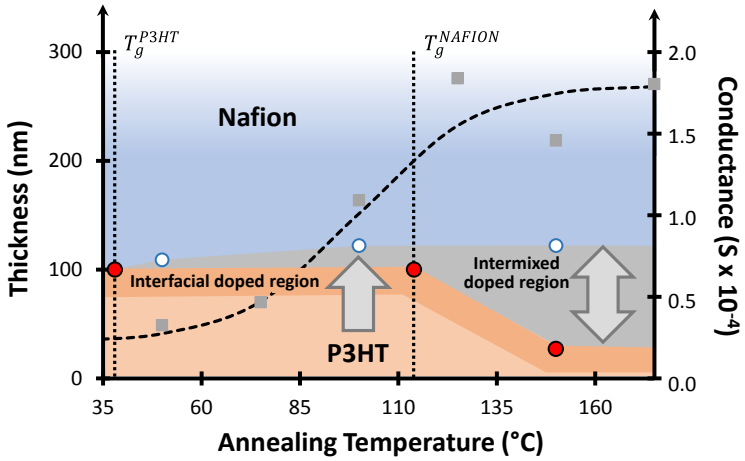

Figure 6. A schematic diagram indicating the doping of P3HT at the P3HT/Nafion interface, and changes to the P3HT/Nafion interface upon thermal annealing, with an associated increase in the effective volume of doped P3HT. The grey squares plot the variation of conductivity with annealing temperature (right axis) with a dashed line added as a guide to the eye. The red and white circles define the thickness of the intermixed doped region (grey shaded region) with annealing temperature (left axis). The dark orange shaded region defines the thickness of the interfacial doped P3HT. The vertical dotted lines at 38 °C and 114 °C denote the T_g values of P3HT and Nafion, respectively.

4. Conclusions

Protic doping in semiconducting polythiophenes/polysulphonic acid bilayers is key to the function of a range of organic electronic devices. Thermal annealing of P3HT:Nafion bilayers produces a discrete intermixed region at the P3HT/Nafion interface arising from a concentration dependent diffusivity of the materials. This intermixed region is protically doped and grows systematically with increasing annealing temperature. This work provides a detailed

model for temperature-modulated doping in P3HT/Nafion bilayers, with important implications for the optimization of organic electronic devices incorporating polythiophene-based polymers with polysulphonic acids. The limitation of this study is that it investigates the electrical behaviour of simple bilayer devices only, rather than integrated OTFT-based sensors. However, these bilayer structures are the platform upon which OTFT-based sensors are built, and studying the fundamental doping mechanism in the platform is necessary in order to make informed decisions when designing and building more complex electronic devices.

Conflicts of Interest

There are no conflicts of interest to declare.

Acknowledgements

This work was performed in part at the Materials Node (Newcastle) of the Australian National Fabrication Facility (ANFF), which is a company established under the National Collaborative Research Infrastructure Strategy to provide nano- and microfabrication facilities for Australia's researchers. This research was supported by the Australian Research Council's Discovery Projects funding scheme (Project DP170102467). H. Andersson (Flinders University) is gratefully acknowledged for GPC measurements. E. Gomez (Penn State University) is gratefully acknowledged for helpful scientific discussion.

Supporting Information

Supporting Information associated with this article can be found in the online version. SEM and optical images of ITO and P3HT/Nafion layers; UV-Vis absorbance spectra of pristine P3HT and pristine Nafion films annealed at temperatures from 50 °C to 250 °C; UV-Vis absorbance spectra of P3HT films immersed in $FeCl_3$ solutions; XPS survey scans of Nafion/P3HT bilayer devices; atomic compositions derived from XPS surface analysis; DMTA temperature scans of Nafion; electrical conductivity calculations.

References

(1) Gu, X.; Shaw, L.; Gu, K.; Toney, M. F.; Bao, Z. The Meniscus-Guided Deposition of Semiconducting Polymers. *Nat. Commun.* **2018**, *9*, 534.

(2) Gu, X.; Zhou, Y.; Gu, K.; Kurosawa, T.; Guo, Y.; Li, Y.; Lin, H.; Schroeder, B. C.; Yan, H.; Molina-Lopez, F.; et al. Roll-to-Roll Printed Large-Area All-Polymer Solar Cells with 5% Efficiency Based on a Low Crystallinity Conjugated Polymer Blend.

Adv. Energy Mater. **2017**, *7*, 1602742.

(3) Andersen, T. R.; Cooling, N. A.; Almyahi, F.; Hart, A. S.; Nicolaidis, N. C.; Feron, K.; Noori, M.; Vaughan, B.; Griffith, M. J.; Belcher, W. J.; et al. Fully Roll-to-Roll Prepared Organic Solar Cells in Normal Geometry with a Sputter-Coated Aluminium Top-Electrode. *Sol. Energy Mater. Sol. Cells* **2016**, *149*, 103–109.

(4) Andersen, T. R.; Larsen-Olsen, T. T.; Andreasen, B.; Böttiger, A. P. L.; Carlé, J. E.; Helgesen, M.; Bundgaard, E.; Norrman, K.; Andreasen, J. W.; Jørgensen, M.; et al. Aqueous Processing of Low-Band-Gap Polymer Solar Cells Using Roll-to-Roll Methods. *ACS Nano* **2011**, *5*, 4188–4196.

(5) Elkington, D.; Belcher, W. J.; Dastoor, P. C.; Zhou, X. J. Detection of Saliva-Range Glucose Concentrations Using Organic Thin-Film Transistors. *Appl. Phys. Lett.* **2014**, *105* (4), 043303.

(6) Elkington, D.; Wasson, M.; Belcher, W.; Dastoor, P. C.; Zhou, X. Printable Organic Thin Film Transistors for Glucose Detection Incorporating Inkjet-Printing of the Enzyme Recognition Element. *Appl. Phys. Lett.* **2015**, *106* (26), 263301.

(7) Griffith, M.; Holmes, N.; Elkington, D. C.; Cottam, S.; Stamenkovic, J.; Kilcoyne, D.; Andersen, T. R. Manipulating Nanoscale Structure to Control Functionality in Printed Organic Photovoltaic, Transistor and Bioelectronic Devices. *Nanotechnology* **2020**, *31*, 092002.

(8) Mabeck, J. T.; Malliaras, G. G. Chemical and Biological Sensors Based on Organic Thin-Film Transistors. *Anal. Bioanal. Chem.* **2006**, *384*, 343–353.

(9) Liao, C.; Yan, F. Organic Semiconductors in Organic Thin-Film Transistor-Based Chemical and Biological Sensors. *Polym. Rev.* **2013**, *53*, 352–406.

(10) Yurash, B.; Cao, D. X.; Brus, V. V.; Leifert, D.; Wang, M.; Dixon, A.; Seifrid, M.; Mansour, A. E.; Lungwitz, D.; Liu, T.; et al. Towards Understanding the Doping Mechanism of Organic Semiconductors by Lewis Acids. *Nat. Mater.* **2019**, *18* (12), 1327–1334.

(11) Mauger, S. A.; Glasser, M. P.; Tremolet de Villers, B. J.; Duong, V. V.; Ayzner, A. L.; Olson, D. C. Doped Interlayers for Improved Selectivity in Bulk Heterojunction Organic Photovoltaic Devices. *Adv. Mater. Interfaces* **2016**, *3* (2), 1500346.

(12) Nam, S.; Kim, J.; Lee, H.; Kim, H.; Ha, C. S.; Kim, Y. Doping Effect of Organosulfonic Acid in Poly(3-Hexylthiophene) Films for Organic Field-Effect Transistors. *ACS Appl. Mater. Interfaces* **2012**, *4* (3), 1281–1288.

(13) Kaake, L. G.; Paulsen, B. D.; Frisbie, C. D.; Zhu, X. Y. Mixing at the Charged Interface of a Polymer Semiconductor and a Polyelectrolyte Dielectric. *J. Phys. Chem. Lett.* **2010**, *1* (5), 862–867.

(14) Liu, C. C.; Yang, C. M.; Liu, W. H.; Liao, H. H.; Horng, S. F.; Meng, H. F. Interface Effect of Oxygen Doping in Polythiophene. *Synth. Met.* **2009**, *159* (12), 1131–1134.

(15) Holmes, N. P.; Burke, K. B.; Sista, P.; Barr, M.; Magurudeniya, H. D.; Stefan, M. C.; Kilcoyne, A. L. D.; Zhou, X.; Dastoor, P. C.; Belcher, W. J. Nano-Domain Behaviour in P3HT:PCBM Nanoparticles, Relating Material Properties to Morphological Changes. *Sol. Energy Mater. Sol. Cells* **2013**, *117*, 437–445.

(16) Dubey, M.; Brison, J.; Grainger, D. W.; Castner, D. G. Comparison of Bi1+, Bi3+ and C60+ Primary Ion Sources for ToF-SIMS Imaging of Patterned Protein Samples. *Surf. Interface Anal.* **2011**, *43* (1–2), 261–264.

(17) Sharma, A.; Pan, X.; Campbell, J. A.; Andersson, M. R.; Lewis, D. A. Unravelling the Thermomechanical Properties of Bulk Heterojunction Blends in Polymer Solar Cells. *Macromolecules* **2017**, *50*, 3347–3354.

(18) Wang, C.; Duong, D. T.; Vandewal, K.; Rivnay, J.; Salleo, A. Optical Measurement of Doping Efficiency in Poly(3-Hexylthiophene) Solutions and Thin Films. *Phys. Rev. B - Condens. Matter Mater. Phys.* **2015**, *91*, 085205.

(19) Scholes, D. T.; Yee, P. Y.; Lindemuth, J. R.; Kang, H.; Onorato, J.; Ghosh, R.; Luscombe, C. K.; Spano, F. C.; Tolbert, S. H.; Schwartz, B. J. The Effects of Crystallinity on Charge Transport and the Structure of Sequentially Processed F4TCNQ-Doped Conjugated Polymer Ffilms. *Adv. Funct. Mater.* **2017**, *27*, 1702654.

(20) Pingel, P.; Neher, D. Comprehensive Picture of P-Type Doping of P3HT with the Molecular Acceptor F4TCNQ. *Phys. Rev. B - Condens. Matter Mater. Phys.* **2013**, *87*, 115209.

(21) Yamamoto, J.; Furukawa, Y. Electronic and Vibrational Spectra of Positive Polarons and Bipolarons in Regioregular Poly(3-Hexylthiophene) Doped with Ferric Chloride.

J. Phys. Chem. B **2015**, *119* (13), 4788–4794.

(22) Paul, D. K.; Karan, K.; Docoslis, A.; Giorgi, J. B.; Pearce, J. Characteristics of Self-Assembled Ultrathin Nafion Films. *Macromolecules* **2013**, *46*, 3461−3475.

(23) Wang, X.; Ederth, T.; Inganas, O. In Situ Wilhelmy Balance Surface Energy Determination of Poly(3-Hexylthiophene) and Poly(3,4-Ethylenedioxythiophene) During Electrochemical Doping-Dedoping. *Langmuir* **2006**, *22*, 9287–9294.

(24) Jung, H.-Y.; Kim, J. W. Role of the Glass Transition Temperature of Nafion 117 Membrane in the Preparation of the Membrane Electrode Assembly in a Direct Methanol Fuel Cell (DMFC). *Int. J. Hydrogen Energy* **2012**, *37*, 12580–12585.

(25) Hansson, R.; Ericsson, L. K. E.; Holmes, N. P.; Rysz, J.; Opitz, A.; Campoy-Quiles, M.; Wang, E.; Barr, M. G.; Kilcoyne, A. L. D.; Zhou, X.; et al. Vertical and Lateral Morphology Effects on Solar Cell Performance for a Thiophene–Quinoxaline Copolymer:PC70BM Blend. *J. Mater. Chem. A* **2015**, *3*, 6970–6979.

(26) Crank, J. *The Mathematics of Diffusion*, 2nd ed.; Clarendon Press: Oxford, 1975.

(27) Sauer, F.; Freise, V. Diffusion in Binären Gemischen Mit Volumenänderung. *Zeitschrift für Elektrochemie* **1962**, *66*, 353–363.

(28) Kodentsov, A.; Paul, A. Chapter 6 - Diffusion Couple Technique: A Research Tool in Materials Science. In *Handbook of Solid State Diffusion*; Paul, A., Divinski, S., Eds.; Elsevier: Amsterdam, 2017; pp 207–275.

(29) Perea, J. D.; Langner, S.; Salvador, M.; Sanchez-Lengeling, B.; Li, N.; Zhang, C.; Jarvas, G.; Kontos, J.; Dallos, A.; Aspuru-Guzik, A.; et al. Introducing a New Potential Figure of Merit for Evaluating Microstructure Stability in Photovoltaic Polymer-Fullerene Blends. *J. Phys. Chem. C* **2017**, *121* (33), 18153–18161.

(30) Choi, P.; Jalani, N. H.; Datta, R. Thermodynamics and Proton Transport in Nafion - I. Membrane Swelling, Sorption, and Ion-Exchange Equilibrium. *J. Electrochem. Soc.* **2005**, *152* (3), E84–E89.

(31) Mana, C. D.; Tomba, J. P. Tracking High Molecular Weight Polymer Interdiffusion on a SERS-Based Platform. *J. Raman Spectrosc.* **2017**, *48* (3), 425–431.

(32) Ludvigsson, M.; Lindgren, J.; Tegenfeldt, J. FTIR Study of Water in Cast Nafion

Films. *Electrochim. Acta* **2000**, *45* (14), 2267–2271.

(33) The Code to Implement the Calculation Is Provided on Zenodo (Https://Doi.Org/10.5281/Zenodo.3957224).

(34) Alveroglu, E. Doping Effect of Dodecyl Benzene Sulphonic Acid in Poly(3-Hexylthiophene)-P3HT-Films. *J. Mol. Struct.* **2015**, *1086*, 86–92.

(35) Duong, D. T.; Wang, C.; Antono, E.; Toney, M. F.; Salleo, A. The Chemical and Structural Origin of Efficient P-Type Doping in P3HT. *Org. Electron.* **2013**, *14* (5), 1330–1336.

(36) Neusser, D.; Malacrida, C.; Kern, M.; Gross, Y. M.; Van Slageren, J.; Ludwigs, S. High Conductivities of Disordered P3HT Films by an Electrochemical Doping Strategy. *Chem. Mater.* **2020**, *32*, 6003−6013.

(37) Marcus, Y.; Hefter, G. Ion Pairing. *Chem. Rev.* **2006**, *106* (11), 4585–4621.

For Table of Contents Only